Supporting Information

Development of a Multifunctional Aminated Zr/Ce Bimetallic MOF-Assisted Membrane for Suppressing Radical-Induced Deterioration in Hydrogen Fuel Cells

*Sk Miraz Hossain[a,c], Vanshita Goyal[a,c], Pratyush Patnaik[a,c], Suman Sarkar[a,c], Santoshkumar D. Bhat[b,c] Uma Chatterjee[a,c],**

[a]*Membrane Science and Separation Technology Division, CSIR-Central Salt and Marine Chemicals Research Institute, Bhavnagar, 364002, India*

[b]*CSIR–Central Electrochemical Research Institute – Madras Unit, CSIR Madras complex, Taramani, Chennai 600113, India*

[c]*Academy of Scientific and Innovative Research (AcSIR), Ghaziabad, 201002, India*

Corresponding author: Uma Chatterjee (umac@csmcri.org, umac.csmcri@csir.res.in)

SI 1. Material

2-Aminoterephthalic acid (ATA) (TCI, India), zirconium (IV) chloride ($ZrCl_4$, TCI, India), N, N-dimethylformamide (DMF, SRL Chemicals India), dichloromethane (DCM, SRL Chemicals India) and N, N-dimethylacetamide (DMAc, SRL Chemicals, India) were used as received. Deuterated dimethyl sulfoxide (DMSO-d_6, 99.9%) was procured from Merck. Cerium nitrate hexahydrate ($Ce(NO_3)_3 \cdot 6H_2O$, Merck), cerium ammonium nitrate (CAN, Merck) ferrous sulfate heptahydrate ($FeSO_4 \cdot 7H_2O$, Molychem, India), hydrogen peroxide (H_2O_2, 30%), sodium chloride (NaCl), and sodium hydroxide (NaOH), all analytical grade, (Qualigens, India) were employed for synthesis and radical tests. Nitric acid (HNO_3, 69%, Research Lab, India) and hydrochloric acid (HCl, 37%, Qualigens, India) were also used in various synthetic steps. Sulfonated poly(ether ether ketone) (sPEEK) polymer fibers (Fumion® E-600, IEC ≈ 1.65 meq g^{-1}, Mw = 50,000 g mol^{-1}, Mn = 14,000 g mol^{-1}) were acquired from FuMA-TECH BWT GmbH, Germany. Fuel cell components including gaskets, platinum catalyst (DURACarb®40 wt% Pt on Vulcan XC72), gas diffusion layers (GDLs), and other accessories were procured from Sainergy Fuel Cell India Pvt. Ltd. Ultrapure water was used throughout all experiments.

SI 2. Synthesis of CeO_2 NPs

Cerium oxide (CeO_2) nanoparticles were synthesized via a modified alkali-assisted precipitation method. Briefly, 2.5 g (4.56 mmol) of CAN was dissolved in 50 mL of 0.1 M HNO_3 and stirred at 70 °C for 2 h. A 0.05 M NaOH solution was then added dropwise under continuous stirring until the pH reached 11–12, resulting in the gradual formation of a pale-yellow precipitate. The suspension was transferred into a 50 mL Teflon-lined stainless-steel autoclave and subjected to hydrothermal treatment at 180 °C for 12 h. Then, the reaction mixture was allowed to digest at ambient conditions for 24 h. Afterwards, the supernatant was decanted, and the precipitate was washed repeatedly with deionized water to eliminate residual ions. The dispersion was centrifuged six times at 7000 rpm until a neutral pH was achieved. The final product was dried under vacuum at 80 °C and ground into a fine powder for further characterization and application.

SI 3. Synthesis of $CeZrO_x$ NPs

Cerium-zirconium bimetallic oxide ($CeZrO_x$) nanoparticles were synthesized via a co-precipitation-assisted hydrothermal method. Equimolar amounts of ($Ce(NO_3) \cdot 6H_2O$) and $ZrCl_4$ were each dissolved in 25 mL of ultrapure water to yield clear solutions with a metal precursor concentration of 0.12 M (3 mmol). The two solutions were then combined under continuous stirring to obtain a homogeneous mixed-metal precursor solution. Subsequently, 0.05 M NaOH was added dropwise at 100 °C until the pH reached 11-12, as monitored using a calibrated pH meter. The alkaline environment induced the gradual precipitation. The resulting suspension was transferred to a 50 mL Teflon-lined stainless-steel autoclave and subjected to hydrothermal treatment at 180 °C for 24 h to promote crystallization and phase development. After natural cooling to room temperature, the mixture was diluted with ultrapure water and allowed to digest for 72 h to enhance structural integrity and crystallinity. The precipitate was subsequently separated and purified through repeated centrifugation at 10,000 rpm using ethanol and deionized water until a neutral pH was attained. The purified $CeZrO_x$ nanoparticles were then collected for further characterization and application.

SI 4. Synthesis of (Zr)U(NH_2) MOF

For comparative analysis, UIO-66-NH_2 MOF, denoted as (Zr)U(NH_2), was synthesized using a solvothermal method. Briefly, 3.06 mmol (750 mg) of $ZrCl_4$ and 0.382 mmol (70 mg) of ATA were dissolved in 30 mL of DMF. To this solution, 7 mL of formic acid was added, serving as both a modulator and a reductant. The mixture was subjected to ultrasonication for 30 minutes to ensure complete dissolution and homogenization. The resulting clear solution was then transferred into a 50 mL Teflon-lined stainless-steel autoclave and heated at 120 °C for 12 h under static conditions. After the reaction, the white precipitate formed was collected by filtration and washed thoroughly with DMF to remove unreacted linkers and residual reactants. Subsequently, the sample was soaked in a mixture of DCM and methanol to promote solvent exchange. The material was then separated by centrifugation at 7000 rpm for 10 minutes and dried at 70 °C for 12 h to obtain the final (Zr)U(NH_2) product for further characterization.

SI 5. Synthesis of (Zr/Ce)U(NH_2) UN MOF under reflux condition

To enable scalable production, a reflux-based synthesis approach was adopted while maintaining the same equimolar stoichiometry of precursors and employing formic acid as both a modulator and mild reductant. In this method, 10 mmol (2.34 g) of $ZrCl_4$, 10 mmol (1.81 g) of BDC-NH_2, and 10 mmol (3.26 g) of $Ce(NO_3)_3 \cdot 6H_2O$ were dissolved in 350 mL of DMF. Subsequently, 1 mol of formic acid was introduced into the solution. The mixture was vigorously stirred to ensure complete dissolution and homogeneity, followed by heating under reflux at 120 °C for 12 h with continuous stirring. Upon completion of the reaction, a white precipitate was obtained from the reaction mixture. The solid product was isolated and purified.

SI 6. Characterization

SI 6.1 Scanning Electron Microscopy (SEM), Atomic Force Microscopy (AFM), and Transmission Electron Microscopy (TEM) analysis of (Zr/Ce)U(NH_2) MOF *and the PEMs*

The surface morphology of the (Zr/Ce)U(NH_2) MOF and the composite proton exchange membranes (PEMs) was investigated using field emission scanning electron microscopy (FE-SEM, JEOL JSM-7100F) operated at an accelerating voltage of 15 kV. AFM analysis of the composite membranes was performed in semi-contact mode using an Ntegra Aura system (NT-MDT, Moscow) under ambient conditions at RT. Image acquisition and processing were carried out using the "Nova" software, with multiple regions of each sample imaged to ensure surface uniformity and reproducibility. For AFM sample preparation, 10 mg of each composite PEM was dissolved in 10 mL of DMAc to prepare a 0.1% w/v solution. After complete dissolution, the solution was drop-cast onto freshly cleaved mica substrates and kept in a $CaCl_2$-filled desiccator with an outlet for 12 h to allow slow solvent evaporation while minimizing moisture exposure. The coated mica samples were then vacuum-dried at 60 °C for an additional 12 h before AFM imaging. TEM analysis of the (Zr/Ce)U(NH_2) MOF was performed using a JEM 2100 (JEOL) instrument operated at an accelerating voltage of 80 kV. For TEM sample preparation, 4 mg of (Zr/Ce)U(NH_2) was dispersed in 15 mL of isopropanol via ultrasonication. The resulting dispersion was drop-cast onto carbon-coated copper grids (SPI Supplies, 300 mesh) and placed in a $CaCl_2$-filled desiccator to ensure slow solvent evaporation and prevent moisture absorption. The grids were subsequently dried under vacuum at 80 °C for 12 h prior to imaging.

SI 6.2. Attenuated Total Reflection Infrared (ATR-IR) spectroscopies

The prepared PEMs were dried in a vacuum oven at 70 °C for 24 h prior to analysis. Membrane samples of approximately 3×3 cm^2 were used for ATR-IR spectroscopy. Similarly, the synthesized (Zr/Ce)U(NH_2) MOF was dried at 70 °C for 12 h before measurement. ATR-IR spectra were recorded at RT using a PerkinElmer instrument equipped with a germanium crystal ATR accessory, fixed at a 45° angle of incidence, providing an approximate penetration depth of ~1 μm in the infrared region. Spectra were collected from five different regions of each sample to ensure reproducibility and sample uniformity.

SI 6.3 Wide-angle XRD of the (Zr/Ce)U(NH_2) MOF and (Zr)U(NH_2) MOF

Wide-angle XRD of (Zr/Ce)U(NH_2) MOF and (Zr)U(NH_2) nanostructure was determined in a powder XRD (Empyrean-PANalytical) instrument using a Cu K_α X-ray source operating at 40 kV and 20 mA with a scan rate of 0.033 °min^{-1} in the 2θ range 5° to 80°.

SI 6.4. X-ray photoelectron spectroscopy (XPS) analysis

(Zr/Ce)U(NH_2) MOF in powder form was dried at 70 °C for 12 h in vacuum. XPS was analyzed for O 1s, N1s, C 2p, Ce 3d, and Zr 3D using Thermo Scientific Nexsa instrument (Al K-Alpha X-rays, 1486.6 eV). X-ray spot size of 400 μm and 100 μm are used for XPS and mapping, respectively. For survey spectra, a pass energy of 200 eV and step size of 1 eV is used. For higher energy resolution, in narrow scan spectra, a pass energy of 50 eV with a step size of 0.1 eV is used. The data was analyzed using Thermo Advantage v5.9925 software and processed using Thermo Advantage v5.9921 software.

SI 6.5 Glass transition temperature (T_g) of the PEMs by DSC analysis

DSC measurements of the PEMs were carried out in a Netzsch DSC 204 F1 Phoenix instrument. The data were analyzed with the help of proteus 6.1.0d software. Cyclohexane and indium were used for the calibration of the temperature scale. Vacuum dried samples (20 mg) were heated from -80 °C to +250 °C at the rate of 20 °C min^{-1}. The samples were then quenched to -80 °C at a rate of 20 °C min^{-1} after keeping it for 1 min at +250 °C and then the second heating was performed at a heating rate of 20 °C min^{-1}. The first run in DSC was necessary to remove the trace of moisture and to the homogenization of the sample. T_g was recorded as the inflection point of the heat-capacity jump from the second heating curve.

SI 6.6 Thermal stability of the PEMs by Thermogravimetric analysis (TGA)

TGA analysis was carried out using a Netzsch TGA (TG209 F1 Libra) system. The membrane samples were heated from 30 °C to 550 °C under a nitrogen atmosphere at a heating rate of 10 °C min^{-1}. The data was analyzed with the help of proteus 6.1.0d software. Similarly, TGA analysis was also performed on the prepared (Zr/Ce)U(NH_2) MOF.

SI 6.7 Characterization of sPEEK by ^1H Nuclear Magnetic Resonance (NMR) spectroscopy

Bruker 600 MHz to spectrometer was used to record the ^1H NMR spectra. ^1H NMR spectra were recorded at 25 °C, using deuterated dimethyl sulfoxide (DMSO-d_6) as solvent and tetramethylsilane (TMS) as the internal reference. The degree of sulfonation (DoS) of sPEEK was determined by analyzing the ^1H NMR spectrum, specifically by calculating the ratio of the integrated area of the proton signal corresponding to the sulfonated aromatic hydrogen ($H_{c'}$) to the total integrated area of all aromatic protons (Fig. S7). The DoS was calculated using the following equation:

$$\frac{n}{12-2n}=\frac{H_{c'}}{\sum H_{a,b,a',b',c,d,e,f,g,h,i,j,k,l}} \qquad (S1)$$

Here, n represents the number of $H_{c'}$ protons per repeat unit.

SI 6.8 Stress-strain property of the PEMs

Stress-strain property (stress and elongation at break) of membrane samples (2.5 cm long, 1 cm width) was determined using ISO 527 S2 method in a Zwick Roell Z2.5 tester. The speed used for the measurement was 20 mm min^{-1}. The testXpert II-V3.5 software was used for data analysis. Measurements were carried out with 4-5 sample films in the water-swollen state, whose averages are reported. During measurements, the water content of the samples was maintained by placing wet tissue around the samples.

SI 6.9 Determination of Water Uptake, Swelling Ratio, and extractable (%) of the PEMs

Three pieces of each type of membrane (dimensions: 3 cm × 3 cm) were dried in a vacuum oven at 70 °C for 24 h to obtain their dry weight (W_d). The dried samples were then immersed in deionized water for 24 h at room temperature. After equilibration, the surface water was gently removed using filter paper, and the wet weight (W_w) was recorded. The water uptake (WU) of the membranes was calculated using the following equation:

$$Water\ uptake\ (\%)=\frac{W_w-W_d}{W_d}\times 100 \qquad (S2)$$

For the determination of swelling ratio, the change of length of the membranes at dry state (L_d) and wet state (L_w) were measured and calculated by the following equation:

$$Swelling\ ratio\ (\%)=\frac{L_w-L_d}{L_d}\times 100 \qquad (S3)$$

SI 6.10 Determination of IEC of the PEMs

The ion exchange capacity (IEC), defined as the amount of exchangeable ionic groups (meq g^{-1}) per unit dry weight of the membrane, was determined using a classical acid–base titration method. Accurately weighed, vacuum-dried membrane samples were immersed in 1 M HCl for 24 h to protonate all available ion exchange sites. The excess acid was then thoroughly rinsed off using deionized water. Subsequently, the membranes were transferred to a 0.5 M

NaCl solution and allowed to equilibrate for 24 h to facilitate the exchange of H^+ ions with Na^+. The released H^+ ions in the solution were titrated against a standardized 0.01 M NaOH solution using phenolphthalein as the pH indicator. At least three ion exchange and regeneration cycles were performed to ensure reproducibility, and the average IEC value over 4–5 cycles is reported. The IEC (in meq g^{-1}) was calculated using the following equation:

$$IEC = \frac{C_{NaOH} \times V_{NaOH}}{Dry\ weight\ of\ PEM} \times \frac{V_{NaCl}}{V'_{NaCl}} \qquad (S4)$$

Where C_{NaOH} and V_{NaOH} are the concentration and volume of NaOH, V_{NaCl} is the volume of NaCl in which the membrane was kept and V'_{NaCl} is the volume NaCl which was used for titration.

SI 6.11 Determination of the proton conductivity of the PEMs

The surface area resistance of the PEMs was evaluated using a through-plane impedance technique employing a potentiostat/galvanostat system (Vionic model, Metrohm Autolab BV, The Netherlands). Membranes were sandwiched between two custom-fabricated acrylic plates equipped with circular carbon electrodes (1 cm diameter; effective area = 1 cm^2), which had been preconditioned in 0.5 M HCl for 12 h and subsequently stored in ultrapure water to maintain hydration. The impedance measurements were performed by applying sinusoidal alternating current over a frequency range of 1 MHz to 1 Hz at a scanning rate of 1 μA s^{-1}. The membrane surface area resistance was extracted from the Nyquist plot by fitting the experimental data using simulation and equivalent circuit modelling. K^m was calculated by using the following equation,

$$\sigma = \frac{\Delta x}{A \times R} \qquad (S5)$$

where Δx is the thickness of the wet membrane, R is the membrane resistance, and A is the effective membrane area.

*SI 6.12***.** *Activation energy (E_a) calculation*

The E_a of the composite PEMs was calculated from their respective Arrhenius plots. The slope of the straight Arrhenius curve (b) was evaluated and the E_a was calculated using the following equation.

$$E_a = -b \times R \qquad (S6)$$

Where b is the slope and R is the gas constant (8.314 KJ $mol^{-1}K^{-1}$).

SI 6.13 Fenton analysis

Fenton's reagent test is a widely adopted method for evaluating the oxidative stability and durability of proton exchange membranes (PEMs) against free radical-induced degradation. It consists of a solution containing 3% H_2O_2 and 3 ppm Fe^{2+}, wherein H_2O_2 reacts with Fe^{2+} to generate highly reactive •OH and •OOH radicals, as depicted in Equations 7 and 8.

$$Fe^{2+} + H_2O_2 \rightarrow Fe^{3+} + \bullet OH + OH^- \qquad (S7)$$

$$Fe^{3+} + H_2O_2 \rightarrow \bullet OOH + Fe^{2+} + H^+ \qquad (S8)$$

This reaction mimics the harsh chemical environment encountered within PEMFCs, where radical formation is triggered by fuel crossover from the cathode to the anode or vice versa. To assess the membrane's resistance to such oxidative stress, samples were immersed in Fenton’s solution at 60 °C for 2 h, with fresh reagent replenished every 2 h to sustain a consistent radical-rich environment. The evaluation was based on monitoring the changes in membrane mass and proton conductivity, which serve as indicators of structural integrity and functional retention under oxidative attack.

SI 6.14 Electrochemical response of the prepared (Zr/Ce)U(NH_2) toward hydroxyl radicals

Cyclic voltammetry (CV) measurements were performed using a conventional three-electrode configuration comprising a glassy carbon electrode (GCE) as the working electrode, a graphite rod as the counter electrode, and an Ag/AgCl electrode as the reference. •OH radicals were generated in situ via the Fenton reaction by mixing equal volumes of 10 mM H_2O_2 and 10 mM $FeSO_4$. To prepare the catalyst ink, 4 mg of Ce-based bimetallic oxide nanoparticles were dispersed in 0.5 mL of isopropanol containing 10 µL of 5 wt% Nafion, followed by ultrasonication for 2 h to obtain a uniform suspension. A 10 µL aliquot of this dispersion was drop-cast onto the GCE surface and dried at 70 °C to ensure firm adhesion. Initial CV scans were recorded in the presence of H_2O_2 over a potential range of -0.8 V to +0.8 V (vs. Ag/AgCl) at a scan rate of 20 mV s^{-1} to evaluate the baseline electrochemical behaviour. Subsequently, after the addition of $FeSO_4$ to initiate •OH radical formation, the CV measurements were repeated under identical conditions. The redox response (ΔA) was determined by calculating the difference between the anodic and cathodic peak currents, normalized to the Ce content of the catalyst.

SI 7. PEMFC studies

SI 7.1 MEA fabrication and PEMFC performance evaluation

The electrochemical performance of the prepared composite membranes was evaluated in PEMFC condition using a test station (Fuel Cell Technologies, Inc.) with an active area of 25 cm^2 (5 cm × 5 cm). The gas diffusion electrode (GDE) was prepared by depositing a Pt catalyst (40 wt% Pt on Vulcan XC-72) onto a commercially available microporous layer - coated gas diffusion layer (GDL). To fabricate the catalyst ink, 50 mg of the Pt catalyst was dispersed in 10 mL of IPA via ultrasonication for 1 h. Subsequently, 30 μL of Nafion® 117 solution (5 wt%) was added as a binder, followed by an additional 30 min of ultrasonication. The resulting homogeneous slurry was brush coated onto the GDL to achieve a catalyst loading of 0.5 mg cm^{-2}. MEA was constructed by sandwiching the composite membrane between two GDEs. The assembly was hot pressed at 90 °C under a pressure of 25 kN cm^{-2} for 3 min. The MEAs were sealed using Teflon gaskets and assembled with moderate torque to ensure proper compression. The cell was operated at 80 °C and 100% relative humidity (RH). Pure H_2 and O_2 gases were supplied to the anode and cathode at flow rates of 100 mL min^{-1} and 150 mL min^{-1}, respectively, through bubble-type humidifiers. Power density curves were recorded, and the measurements were repeated in multiple cycles to ensure reproducibility and data consistency.

SI 7.2 Durability assessment via OCV decay (ADT analysis)

The long-term durability of the MEAs was assessed through an OCV degradation test, following a modified U.S. Department of Energy (DOE) protocol. The OCV was continuously monitored for 100 h at 80 °C and 30% RH. During the test, H_2 and O_2 were supplied to the anode and cathode at 100 mL min^{-1} and 150 mL min^{-1}, respectively. The decline in OCV over time served as an indicator of membrane degradation under accelerated stress conditions.

SI 7.3 Fuel crossover analysis

Fuel (H_2) permeability across the membrane was evaluated both before and after the durability test using LSV in a fuel cell configuration. In this setup, the cathode acted as the working electrode, while the reference and counter electrodes were placed at the anode side. The LSV measurements were conducted in the voltage range of 0 to 0.6 V at a scan rate of 50 mV s^{-1} and 80 °C under humidified conditions. Humidified H_2 and nitrogen (N_2) were supplied to the anode and cathode, respectively, at flow rates of 150 mL min^{-1}. Prior to analysis, the cell was conditioned for 3 h with N_2 gas. The crossover current density was used to quantify H_2 permeability through the membrane, serving as a metric for evaluating structural integrity of the membrane pre and post-ADT conditions.

SI 7.4 Current density and power density calculations

The power density and current density was calculated using the following equations.

$$current\ density = \frac{I}{A} \qquad (S9)$$

$$power\ density = current\ density\ \times V \qquad (S10)$$

Where, I is the current produced using the membrane at a given potential V and A is the electrochemical active area of the fuel cell test station.

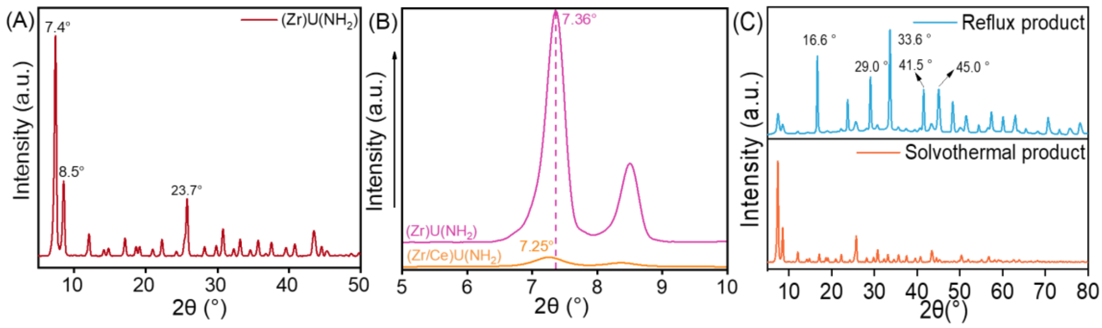

Fig. S1. (A) XRD pattern of (Zr)U(NH_2) MOF, (B) low-angle XRD comparison between (Zr)U(NH_2) and bimetallic (Zr/Ce)U(NH_2) MOFs, (C) comparative XRD profiles of (Zr/Ce)U(NH_2) synthesized via reflux and solvothermal methods.

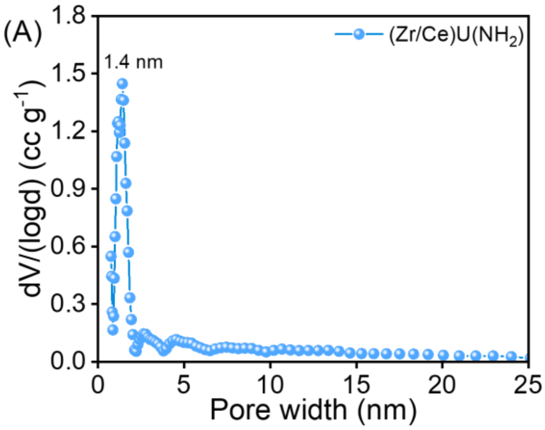

Fig. S2. (A) Pore size distribution curve of the (Zr/Ce)U(NH_2) samples calculated by the BJH method.

(A)

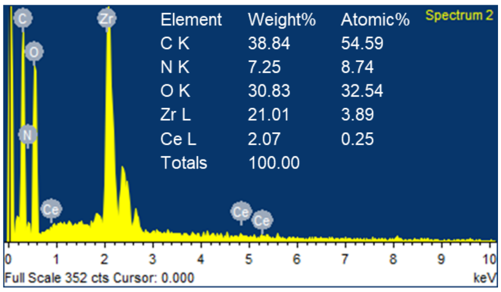

Fig. S3. (A) EDS elemental mapping of the (Zr/Ce)U(NH_2).

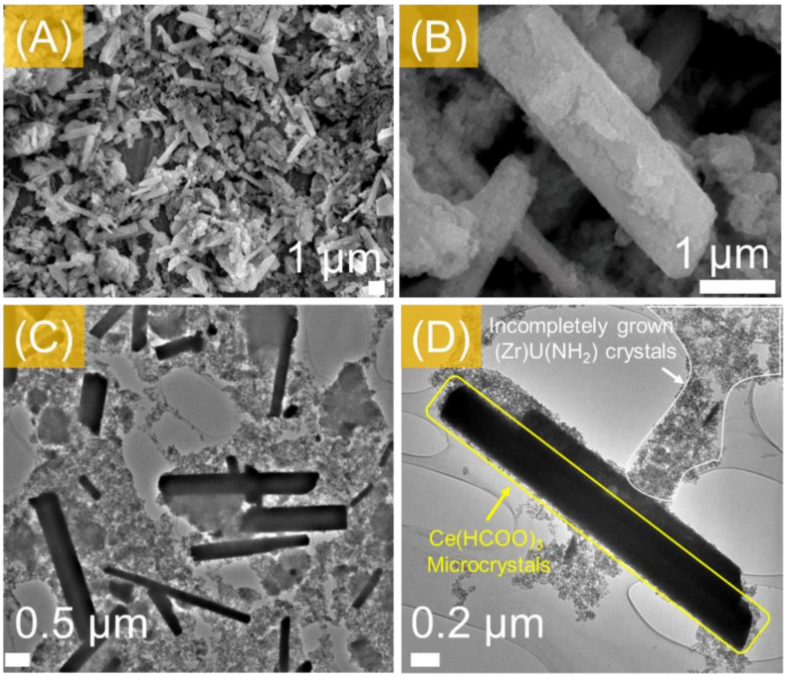

Fig. S4. (A-B) SEM images and (C-D) TEM images of the (Zr/Ce)U(NH_2) MOF synthesized via reflux method.

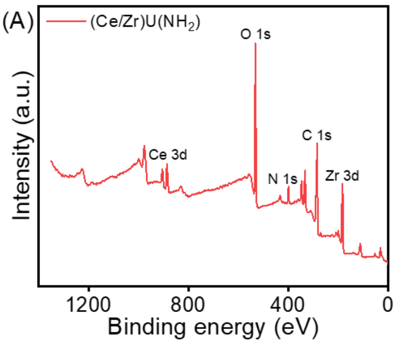

Name	FWHM eV	Atomic %
O1s	3.88	33.41
C1s	4.79	55.96
Zr3d	4.67	3.98
Ce3d5	5.99	0.98
N1s	3.76	5.68

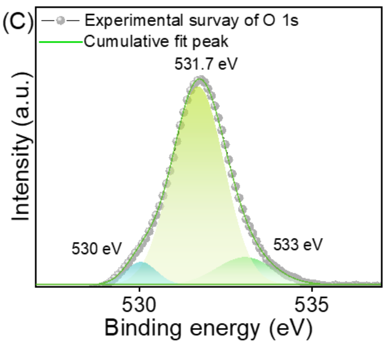

Fig. S5. (A) XPS full survey scan of (Zr/Ce)U(NH_2), (B) peak table, and (C) deconvoluted XPS spectra for O 1s spectra in (Zr/Ce)U(NH_2) MOF.

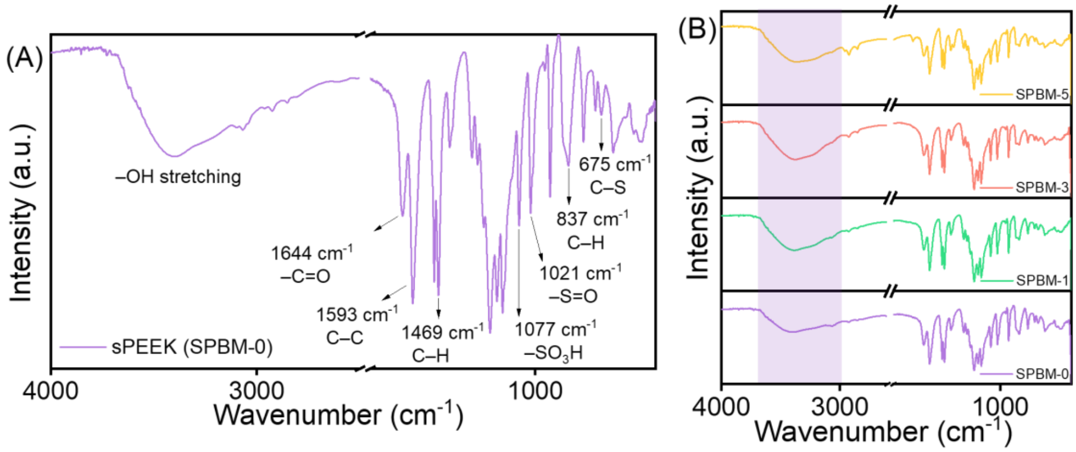

Fig. S6. ATR-IR spectrum of the prepared (A) pristine sPEEK, and (B) composite membranes.

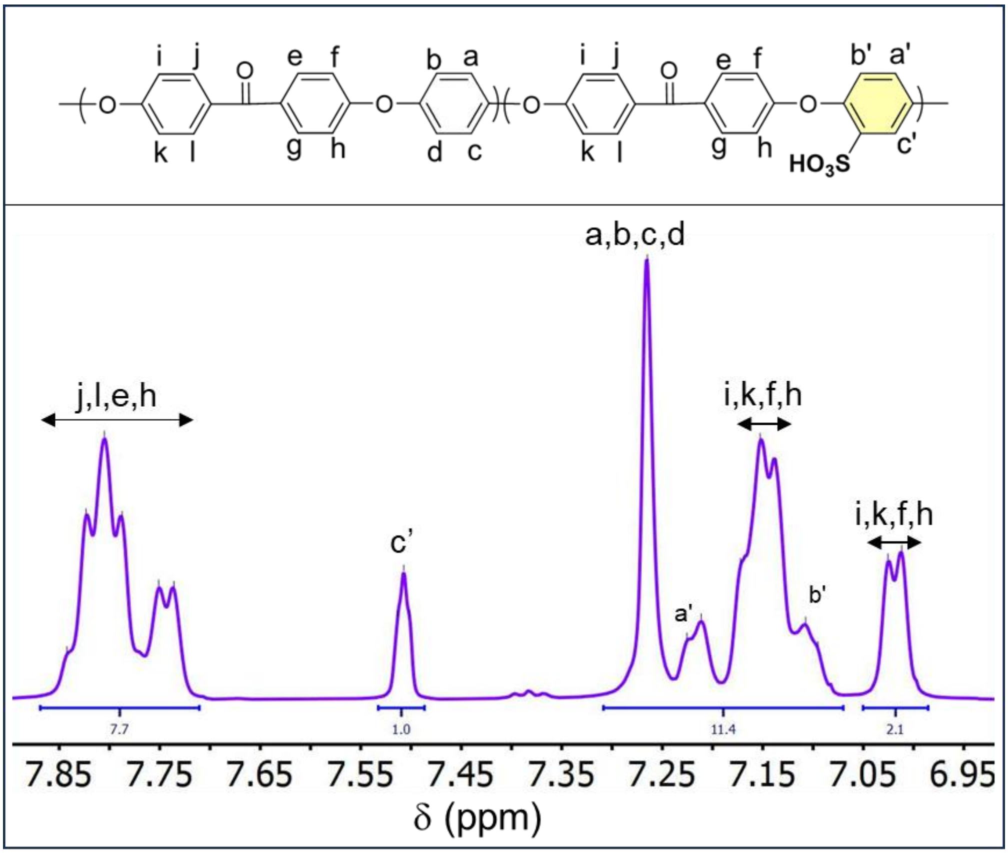

Fig. S7. ^{1}H NMR spectra of sPEEK.

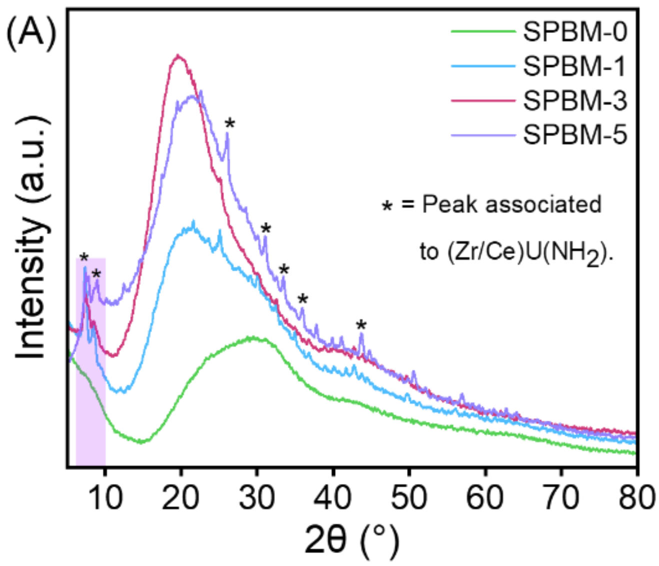

Fig. S8. (A) XRD pattern of the prepared composite membranes.

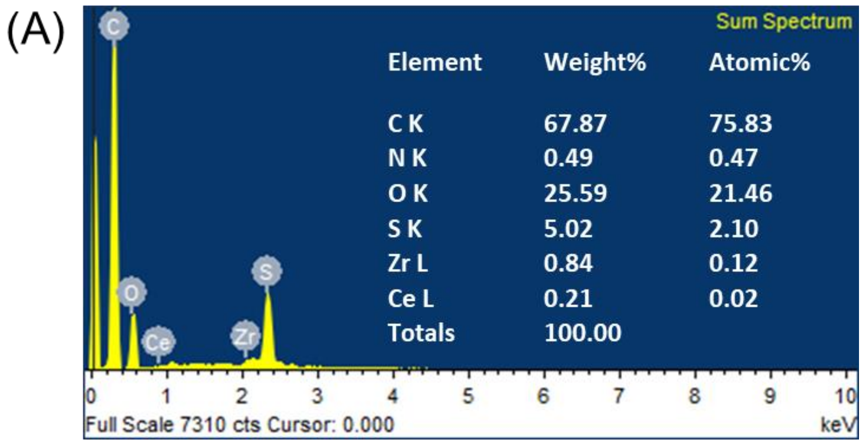

Fig. S9. EDS Elemental mapping of the prepared SPBM-3 membrane.

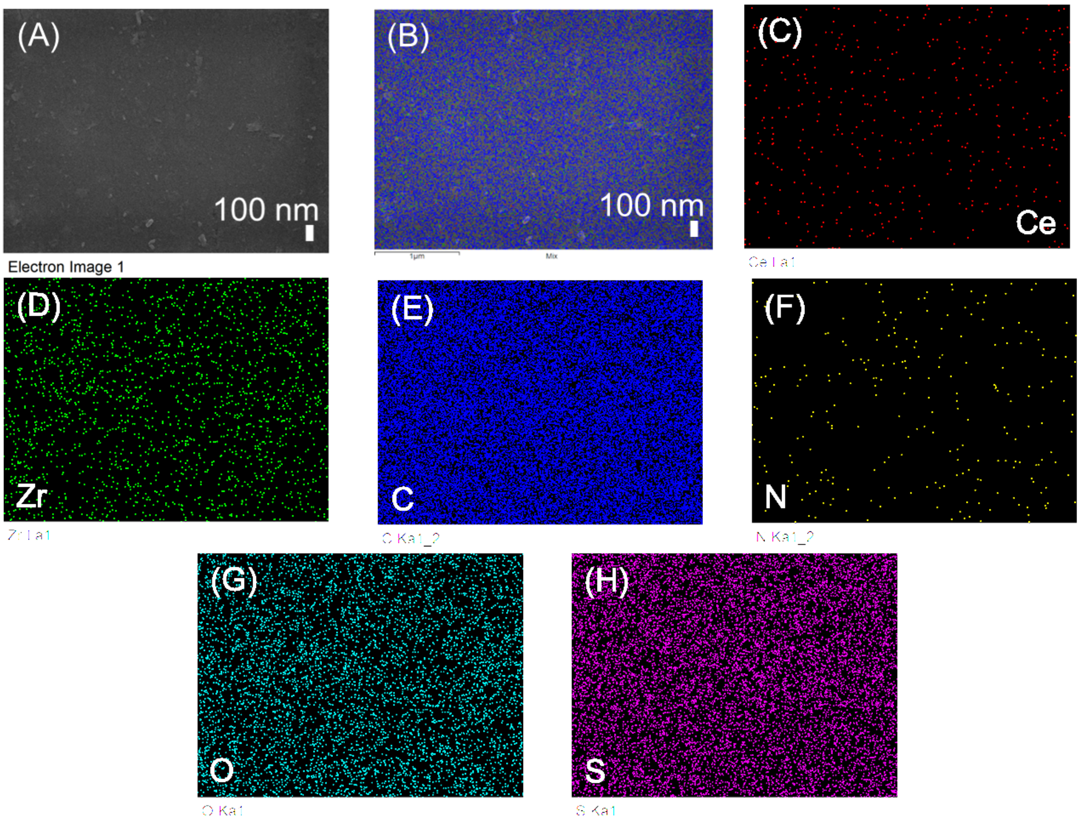

Fig. S10. Elemental mapping showing Ce, Zr C, N, O, and S distribution in the prepared SPBM-3 membrane with the membrane's electronic image.

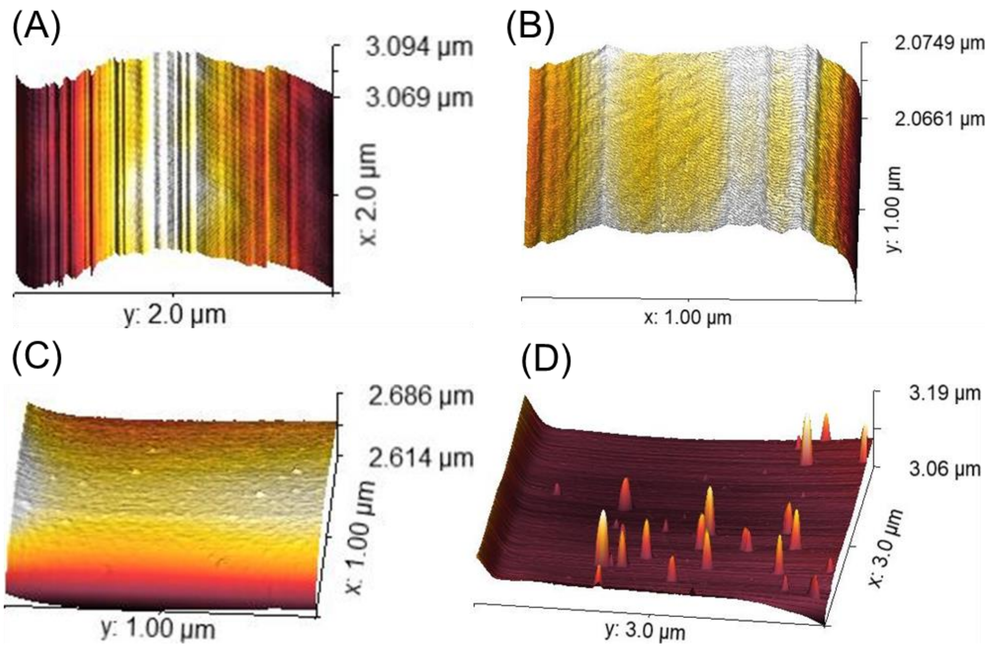

Fig. S11. Topological AFM images of prepared (A) SPBM-0, (B) SPBM-1, (C) SPBM-3, and (D) SPBM-5 membranes.

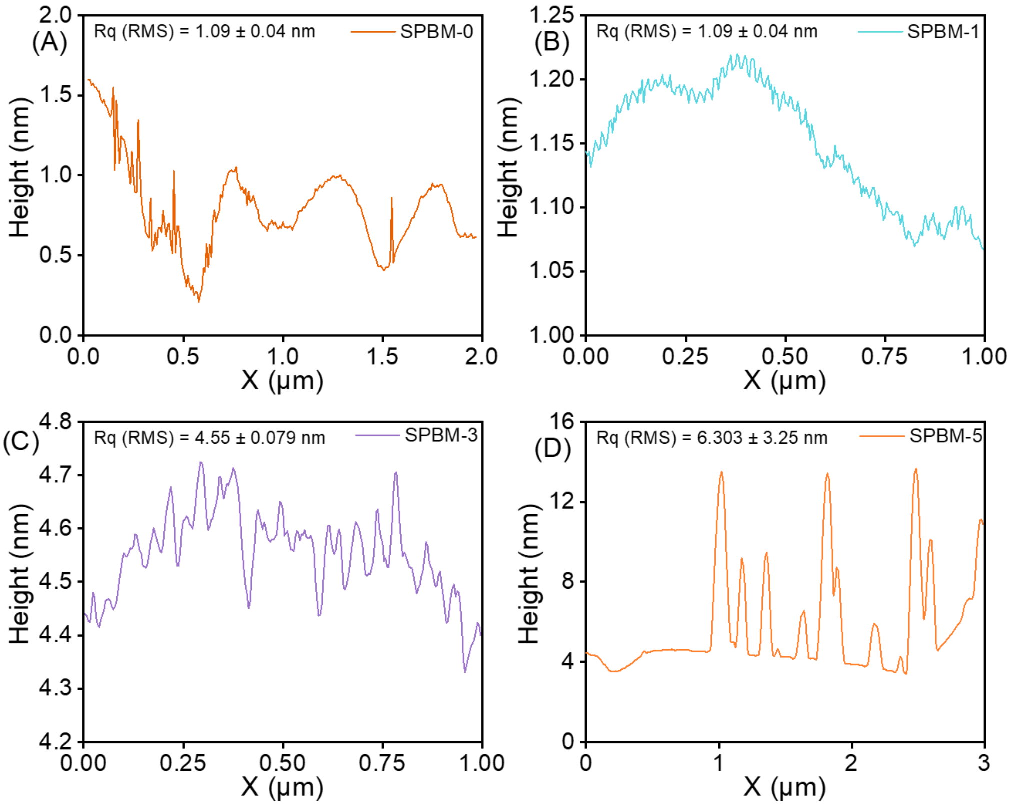

Fig. S12. Surface roughness profile plots of (A) SPBM-0, (B) SPBM-1, (C) SPBM-3, and (D) SPBM-5 membrane.

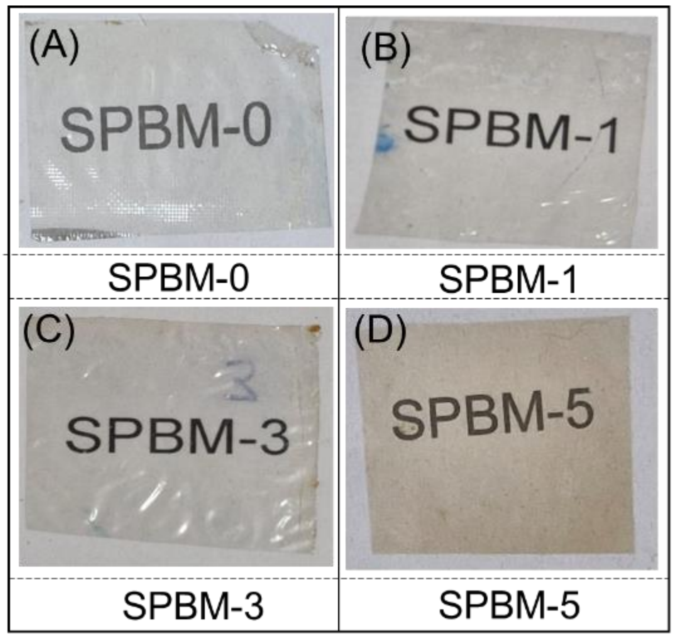

Fig. S13. (A-D**)** Digital images of the prepared PEMs.

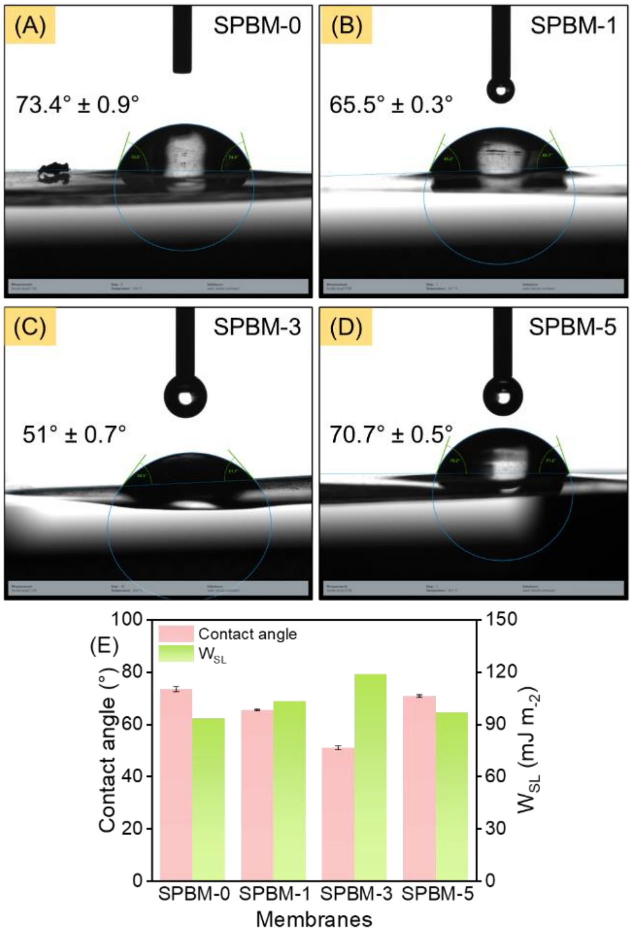

Fig. S14. (A-D) Contact angle measurements and (E) represent the measured θ_{WCA} & W_{SL} values of the prepared PEMs.

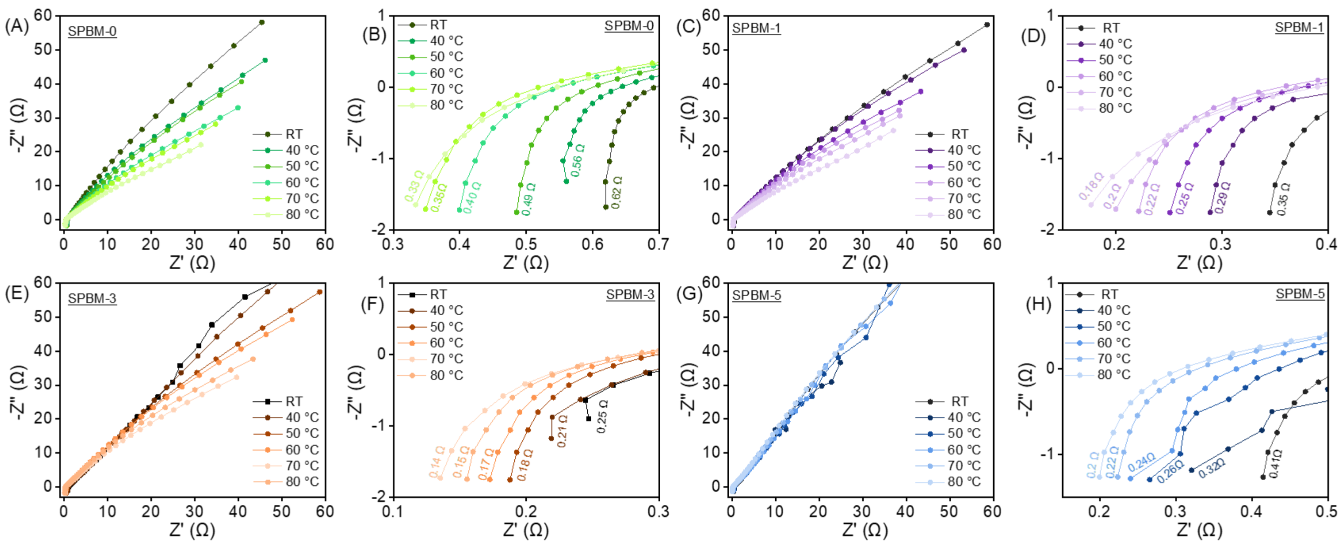

Fig. S15. Nyquist plots of the prepared PEMs recorded over a temperature range from RT to 80 °C.

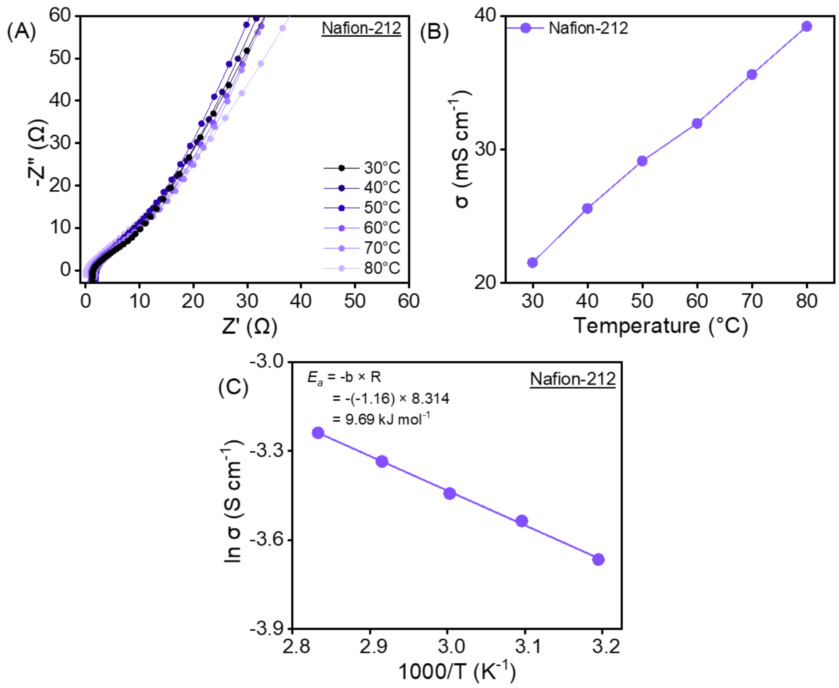

Fig. S16. A) Nyquist plots of the Nafion-212 membrane at various temperatures, (B) enhancement of proton conductivity with temperature, (C) Arrhenius plot to estimate the E_a for proton conduction in Nafion-212.

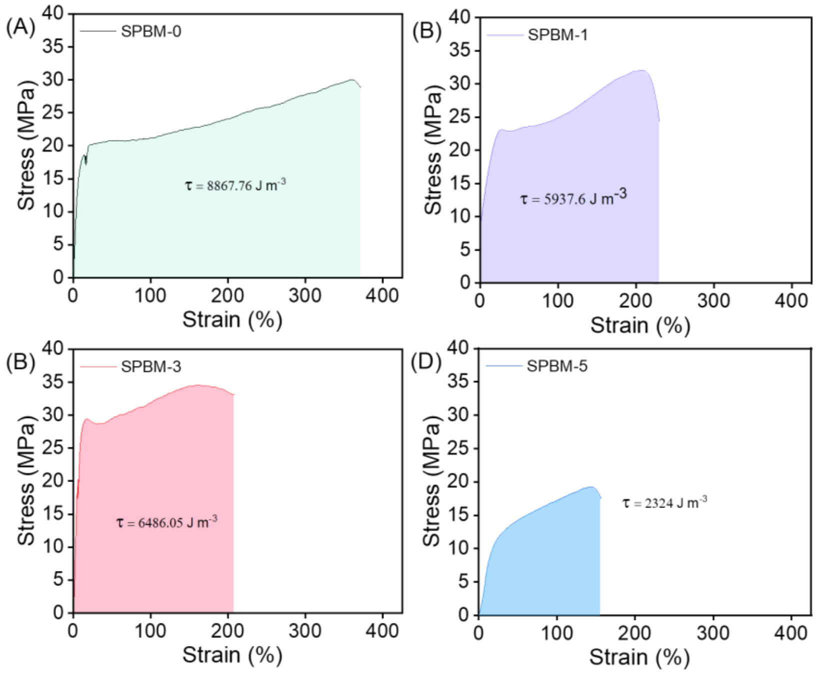

Fig. S17. (A-D) Modulus of toughness (area under the stress-strain curve) of the respective membranes.

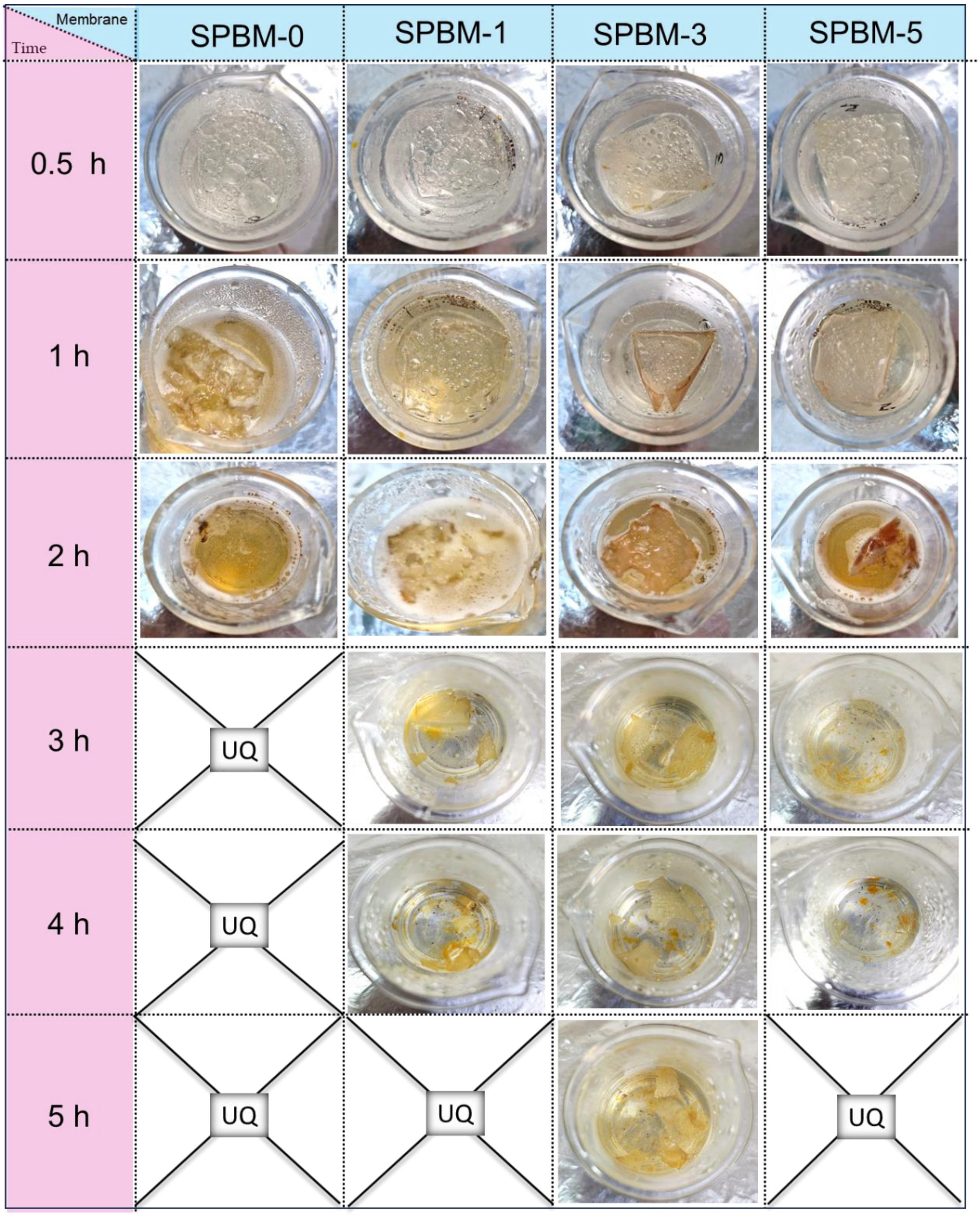

Fig. S18. Digital images of the prepared PEMs at different time intervals during the Fenton test.

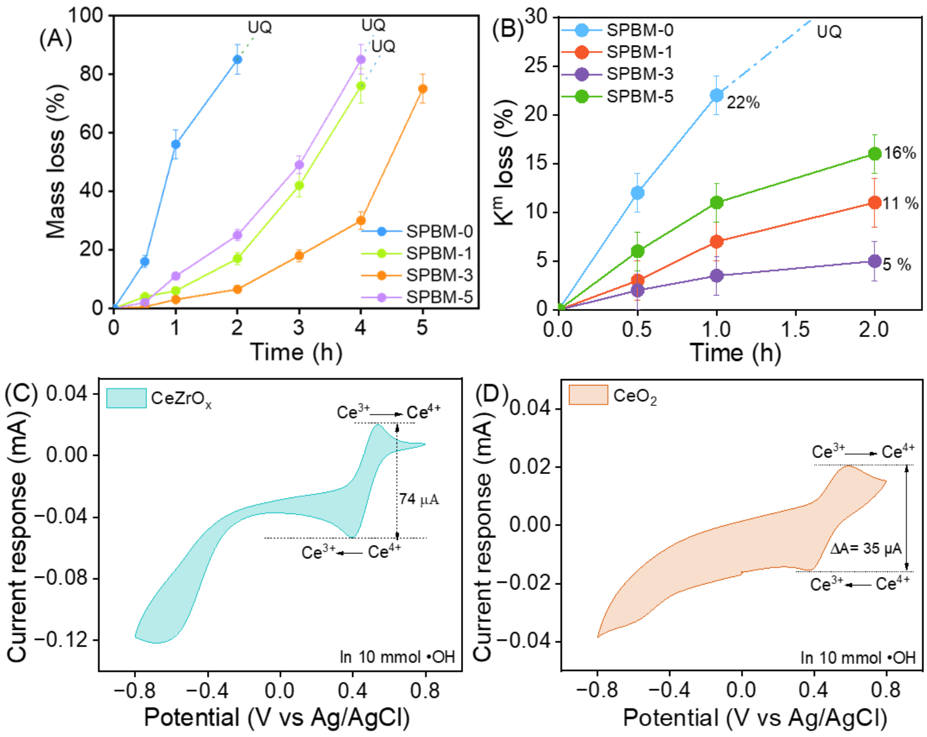

Fig. S19. (A) Mass loss and (b) conductivity loss of the prepared PEMs during Fenton's analysis. CV of the prepared (C) $CeZrO_x$ and (D) CeO_2.

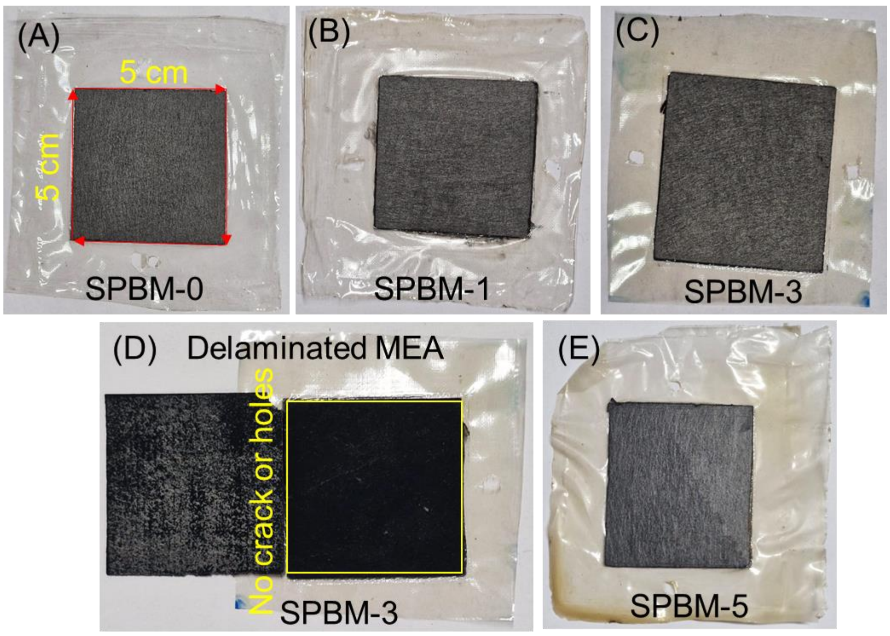

Fig. S20. (A), (B), (C), and (E) are the digital images of the prepared MEAs of SPBM-0, SPBM-1, SPBM-3, and SPBM-5 membrane respectively, (D) deliberately delaminated SPBM-3 MEA showed no cracks or visible degradation.

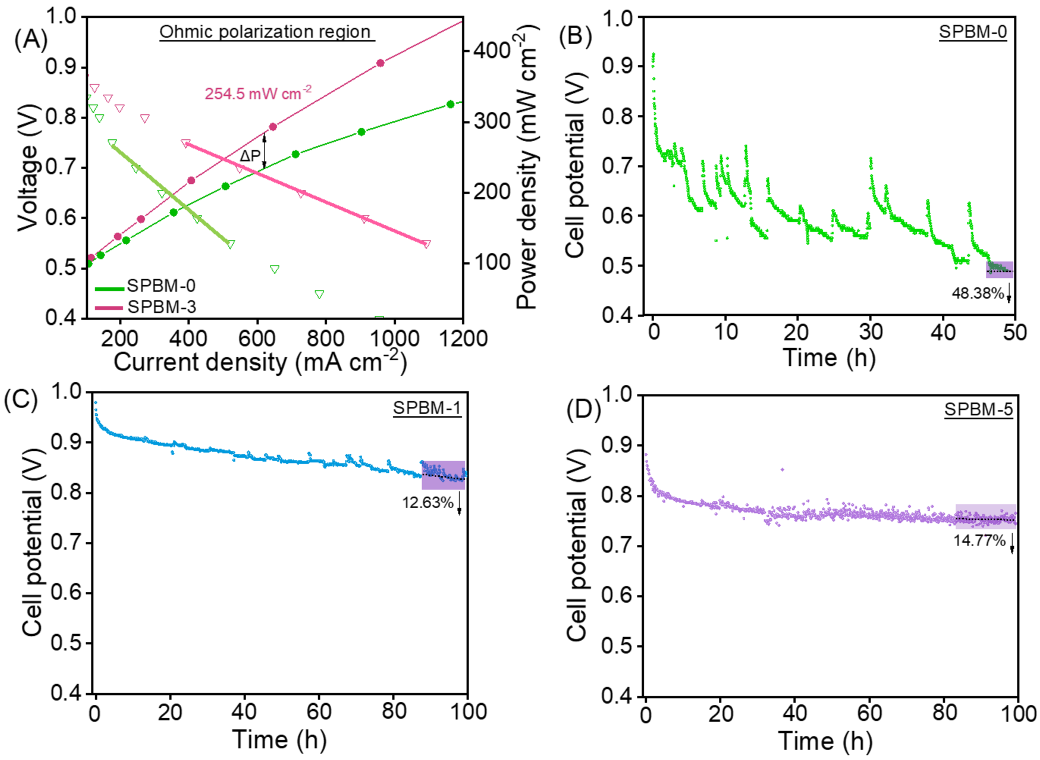

Fig. S21. (A) Average ΔP between SPBM-0 and SPBM-3 in the ohmic polarization region. (B), (C), and (D) are the ADT analysis plot of the prepared MEA of SPBM-0, SPBM-1, and SPBM-5 membrane respectively.

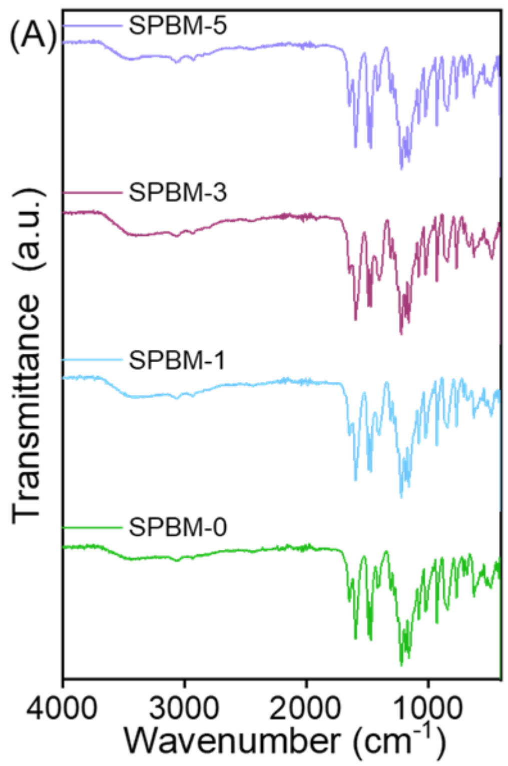

Fig. S22. Post-ADT ATR-IR spectrum of the prepared membranes.

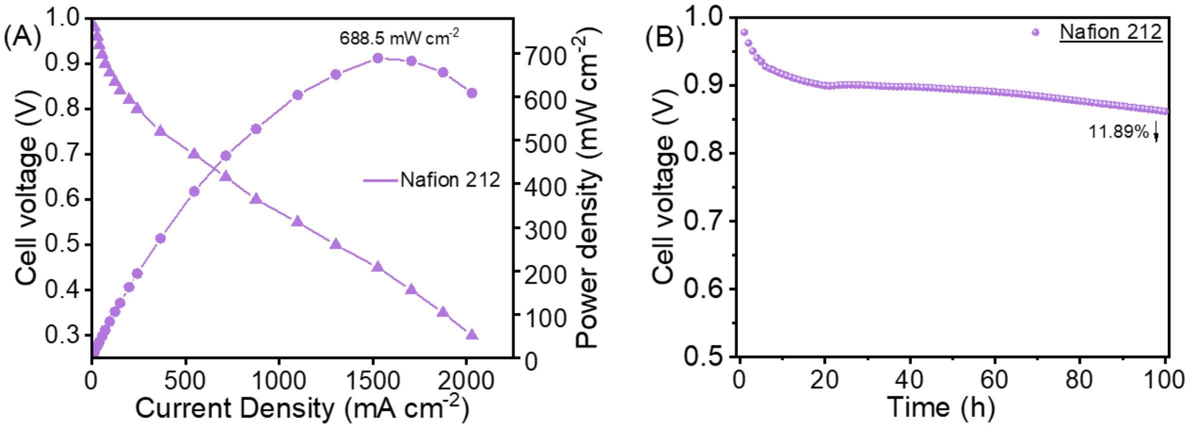

Fig. S23. (A) Single cell fuel cell performance and (B) the ADT analysis of Nafion 212.

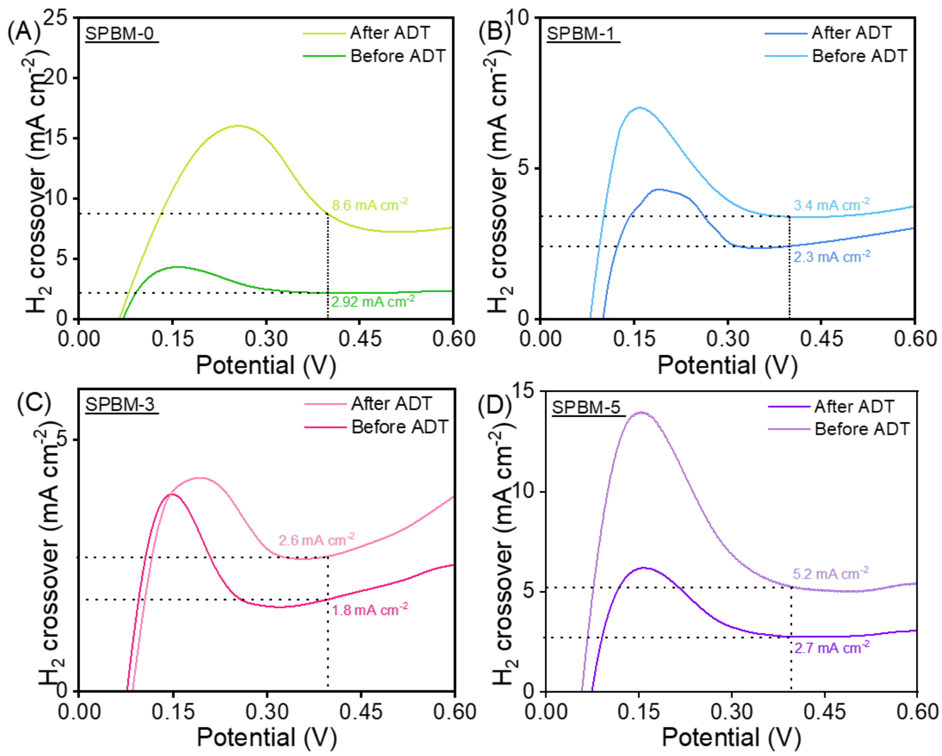

Fig. S24. LSV analysis of the prepared MEA of (A) SPBM-0, (B) SPBM-1, (C)SPBM-3 and (D) SPBM-5 membrane respectively.

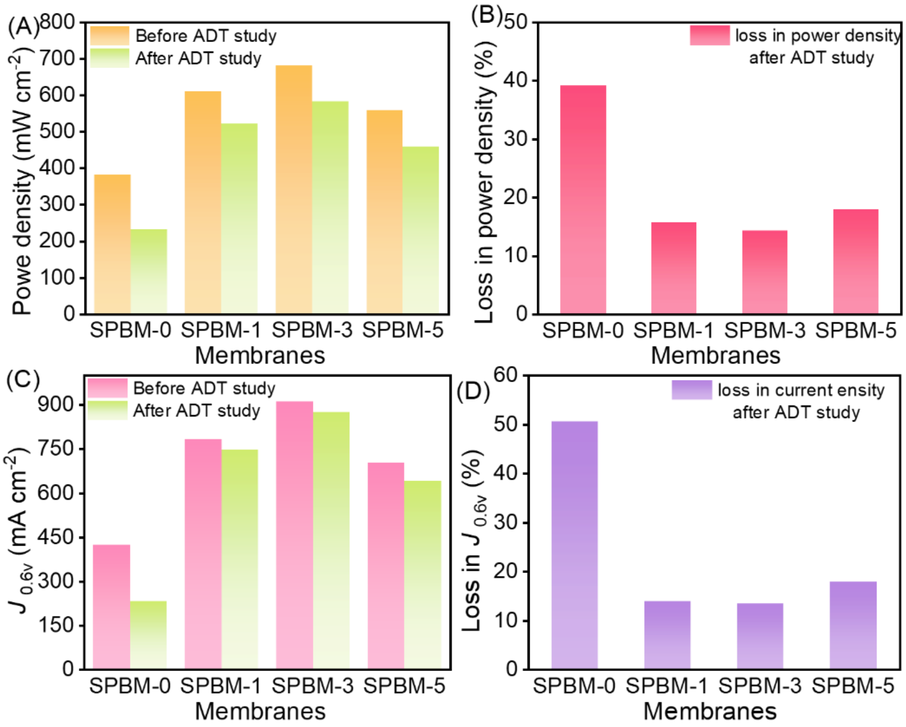

Fig. S25. (A) Comparative P_{max} analysis, (B) loss in P_{max} after ADT analysis, (C) $j_{0.6V}$ values of the prepared membranes, and (D) loss in $j_{0.6V}$ value after ADT analysis.

Cost Calculation for Making 1 Gram (Zr/Ce)U(NH_2)									
Chemicals Required	**FMOF (Lab scale) mmol**	**Molecular Weight (g/mol)**	**Quantity (mg or mL)**	**Quantity required for gram-scale FMOF (mmol)**	**Quantity in g or L**	**Price**	**Price per g or L (A)**	**Company Name**	**Price for gm Scales**
Cerium(III) nitrate hexahydrate	0.386	434.22	167.6 mg	1.61	0.69 g	117.20 $ / 100g	1.17$	Merck	0.81 $
Zirconium(IV) Chloride	0.386	233.02	89.94 mg	1.61	0.14 g	80.22 $ / 100g	0.80$	TCI	0.11 $
2-Aminoterephthalic Acid	0.386	181.15	69.92 mg	1.61	0.11 g	33.99 $ / 25g	1.36$	TCI	0.15 $
Formic Acid	-	46.03	4 mL		16.67 mL	35.49 $ / 300mL	0.12$	TCI	2 $
DMF	-	-	15 mL		62.5 mL	33.99 $ / 2.5L	0.014$	SRL	0.875 $
Total cost for making 1 g (Zr/Ce)U(NH_2)									3.945 $
Total cost for making 100 g (Zr/Ce)U(NH_2)									394.5 $

Fig. S26. Cost calculation for preparing (Zr/Ce)U(NH_2).

Cost Calculation for Fabricating 30×20 cm^2 SPBM-3 membrane				
Chemicals Required	**Quantity required for fabricating 10cm^2 membrane**	**Price**	**Company Name**	**Price per g or L (A)**
Sulfonated poly(ether ether ketone) (sPEEK)	2.4 g	3456.79 $ / 100g	FUMATECH BWT GmbH	82.96 $
DMAc	60 mL	19 $ / 2.5L	SRL	0.46 $
(Zr/Ce)U(NH_2)	0.072	3.95 $ / 1g	CSMCRI	0.28 $
Total cost for fabricating 30×20 cm^2 SPBM-3 membrane				83.7 $

Fig. S27. Cost calculation for SPBM-3 membrane fabrication.

Table S1. Comparison of polarization voltages, power output at current densities for SPBM-0 and SPBM-5 membrane, respectively.

Samples	Potential (V)	Power density ($mW\ cm^{-2}$)	Power Density Increment (ΔP, $mW\ cm^{-2}$)	Average power density increment ($mW\ cm^{-2}$)
SPBM -0	0.55	286.08	314.47	254.48
SPBM -3	0.55	600.55		
SPBM -0	0.60	254.35	292.28	
SPBM -3	0.60	546.63		
SPBM -0	0.65	209.06	263.27	
SPBM -3	0.65	472.33		
SPBM -0	0.70	172.01	211.44	
SPBM -3	0.70	383.45		
SPBM-0	0.75	132.30	160.92	
SPBM-3	0.75	293.22		

Table S2. Comparative evaluation of the prepared PEMs with other reported PEMs containing Ce-based free radical scavengers in terms of OCV decay rate at low RH condition.

No	Membrane	Polyelectrolyte	Antioxidant filler	ADT condition	OCV degradation rate	Ref
1	PFSA/Ce-$BTC_{1.0}$	PFSA	Ce-BTC MOF	90 °C, at 30% RH	0.56 mVh^{-1}	[1]
2	PFSA/Ce-$TPA_{2.0}$	PFSA	Ce-TPA MOF	80 °C, at 50% RH	0.38 mVh^{-1}	[2]
3	Ce complex-1	PFSA	$[Ce(dipic)_3]^{3-}$ complex	90 °C, 30% at RH	0.606 mVh^{-1}	[3]
4	CeO2@TP	PFSA	CeO_2@Tea polyphenols	80 °C, 20% at RH,	0.22 mVh^{-1}	[4]
5	Ce-NH_2BDC@PFSA	PFSA	Ce-NH_2BDC MOF	90 °C, at 30% RH	0.033 mVh^{-1}	[5]
6	SPZr	sPEEK	$CeZrO_x$	80°C, at 30% RH	1.48 mVh^{-1}	[6]
7	SPMn	sPEEK	$CeMnO_x$	80°C, at 30% RH	1.71 mVh^{-1}	[6]
8	SPZn	sPEEK	$CeZnO_x$	80°C, at 30% RH	1.81 mVh^{-1}	[6]
9	SPBM-0	sPEEK	No filler	80°C, at 30% RH	10.17 mVh^{-1}	**This Work**
10	SPBM-3	sPEEK	(Zr/Ce)U(NH_2)	80°C, at 30% RH	1.10 mVh^{-1}	**This Work**

1. K. Xu, G. Liu, X. Xu, Z. Wang, G. Liu, F. Liu, Y. Zhang, Y. Zhou, Y. Zou and S. Pei, *J. Membr. Sci.*, 2024, **699**, 122641.
2. K. Xu, S. Pei, W. Zhang, Z. Han, P. Guan, L. Wang, Y. Zou, H. Ding, X. Ma, C. Xu, F. Liu and Y. Zhang, *Materials Today Energy*, 2023, **31**, 101195.
3. T. Kwon, S. H. Park, B. J. Min, S. Park, S. Ramadhani, Y. Lim, S. S. Jang, H. Jeong, H. J. Son and J. Y. Kim, *Advanced Energy and Sustainability Research*, 2022, **3**, 2200011.
4. S. Zhao, Y. Liao, R. Wang, G. Liu, H. Zhang and H. Tang, *Chem. Eng. J.*, 2023, **472**, 144804.
5. H. Huang, Z. Zhong, J. Li and H. Li, *ACS Applied Energy Materials*, 2024, **7**, 10804-10814.
6. S. M. Hossain, P. Patnaik, S. D. Bhat and U. Chatterjee, *J. Membr. Sci.*, 2025, **728**, 124159.